Enhanced Adhesion between Polypropylene and Polyamide-6: Role of Interfacial Nucleation of the β-Crystalline Form of Polypropylene

Eric Boucher,[†] John P. Folkers,[†] Costantino Creton,[‡] Hubert Hervet,[†] and Liliane Léger*,[†]

Laboratoire de Physique de la Matière Condensée, U.R.A. C.N.R.S. 792, Collège de France, 11, place Marcelin-Berthelot, 75231 Paris Cedex 05, France, and Laboratoire de Physico-chimie Structurale et Macromoléculaire, ESPCI, 10, rue Vauquelin, 75231 Paris Cedex 05, France

Received July 25, 1996; Revised Manuscript Received December 27, 1996[⊗]

ABSTRACT: We present an investigation of the mechanisms of mechanical reinforcement at interfaces between polypropylene (PP) and polyamide-6 (PA6), associated with the incorporation of a small amount of maleic anhydride functionalized PP (PP-*g*-MA) which reacts with the NH_2 groups of the PA6 to form a copolymer in situ. In a previous study we have demonstrated, for one molecular weight of PP-*g*-MA, that diblock copolymer molecules were indeed formed at the interface, with an areal density Σ, controlled by the reaction temperature and the reaction time, and that the measured fracture toughness of the interface scaled as $G_c \propto \Sigma^2$, regardless of the reaction temperature, but for similar sample cooling conditions. We report here the behavior of the same system for a higher molecular weight PP-*g*-MA: at a reaction temperature above 220 °C, very close to the melting point of the PA6, and above a given Σ, the measured G_c becomes 4 times higher than that for reaction temperatures below 220 °C, where the observed G_c values are identical to what has been measured for the low molecular weight PP-*g*-MA. G_c is therefore no longer uniquely dependent on Σ. Crystallographic analysis on the PP side of the interface showed a correlation between the presence of the PP β-phase in the 20 μm near the interface and a high toughness; this crystalline phase was not present in the samples prepared at $T \leq 220$ °C or with the low molecular weight PP-*g*-MA which always exhibited a low toughness even for samples prepared above 220 °C. It is argued that the presence of this β phase of the PP is the main factor responsible for the very high fracture toughness, first evidence of the influence of the crystallinity of a semi crystalline polymer on its adhesive properties.

Introduction

Most polymer pairs are immiscible at the molecular level and, as a result, form two or more phases upon blending. The mechanical properties of such blends depend, among other things, on the structure and mechanical strength of the interface between these different phases. Without additives, this interface is weak due to the lack of entanglements between the chains of both polymers. Therefore, the mechanical reinforcement of the interface between two immiscible polymers is generally achieved by the addition of a third component acting as a molecular connector, entangled on both sides of the interface.[2−7] So far, much of the fundamental work in this area has been devoted to the reinforcement of interfaces between glassy polymers with diblock copolymers,[4,6,8−10] although recently some work with triblock copolymers and random copolymers has appeared.[7,11] The combined development of surface analysis techniques, new micromechanical models, and the wider availability of well-characterized connecting polymers has made possible more fundamental studies, which have produced a well-accepted picture of interfacial failure as a function of such parameters as the areal density of the copolymer at the interface and its molecular weight.[7] Two different relationships between the fracture toughness of the interface (G_c) and the areal density of connecting chains (Σ) have been observed: if failure of the interface occurs by simple chain scission or chain pull-out without any extensive plastic deformation, G_c is a linear function of Σ; if the applied stress at the interface is sufficient to activate bulk plastic deformation mechanisms, then G_c increases significantly and scales with Σ^2.

In a recent study,[1] we began to address the problem of reinforcement between polypropylene (PP) and polyamide-6 (PA6), two immiscible, semicrystalline polymers. In this case, a suitable block copolymer is not readily available and the reinforcement was achieved by *in situ* formation of a diblock copolymer, through the reaction at the interface of an amine terminated PA6 molecule and a PP chain grafted with maleic anhydride. For one particular molecular weight of the copolymer, we have shown that the mechanism of reinforcement was surprisingly similar to that observed for glassy polymers. The copolymer molecules acted as connecting chains and the maximum stress that could be sustained by the interface was sufficient to activate the plastic deformation mechanisms. Dissipation occurred (presumably by the formation of crazelike fibrils) exclusively on the PP side of the interface, and the joints failed ultimately by scission of the PP part of the copolymer. G_c was observed to scale with Σ^2, as for glassy polymers,[9,12] with a comparable prefactor. We thus argued that the model of the micromechanics of a fibrillar plastic zone, recently proposed by Brown,[13] could be applicable to the case of these semicrystalline polymers, and that the general structure of the plastic deformation zone in the PP was able to transfer some stress laterally in a similar way to what happens in a craze in glassy polymers.

It is important to point out that the large measured G_c values are due to the formation of a plastic zone ahead of the propagating crack tip. The fracture tough-

[†] Collège de France.
[‡] ESPCI.
[⊗] Abstract published in *Advance ACS Abstracts,* March 1, 1997.

S0024-9297(96)01105-9 CCC: $14.00

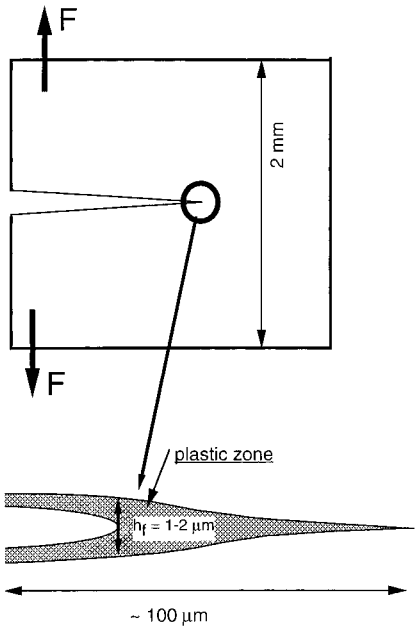

Figure 1. Schematics of the plastic zone at the crack tip.

ness is directly proportional to the maximum width that this plastic zone can achieve, as shown schematically in Figure 1. A simple estimate of the maximum width of this plastic zone can be obtained by dividing the measured G_c by the yield stress of the bulk polymer drawn into the plastic zone. For tough interfaces, the resulting maximum width can be of several microns. This is much larger than the size of the connecting chains themselves (typically 50 nm), and the bulk properties of the polymers on either side of the interface should affect the measured G_c.

One reported example of such an effect in glassy polymers is the case of polystyrene−poly-(2-vinylpyridine) (PS−PVP) block copolymers at the interface between PS and PVP. The incorporation of 25% of miscible poly(phenylene oxide) (PPO) in the bulk PS raises the crazing stress of the PS phase and therefore inhibits the formation of a craze in the PS, resulting in a lower fracture toughness than when the homopolymer is pure bulk PS.[14]

In semicrystalline polymers, a change in the crystalline structure or in the macrostructure of the crystallinity can have profound effects on the plastic deformation properties of the polymer.[15−18] If, as argued above, the fracture toughness G_c is affected by the yield stress of the polymer undergoing the plastic deformation, we can expect that not only Σ but also the crystalline microstructure and macrostructure near the interface should affect the measured value of the fracture toughness. We present here experimental evidences that this is indeed the case for the PP−PA6 system.

Experimental Section

Materials. Commercial-grade polyamide-6 (PA6) with M_n = 17 000 and a polydispersity index PDI = 2 was obtained from BASF and had an average of one NH_2 end per chain. Commercial-grade polypropylene (PP) with M_n = 57 000 and PDI = 4.8 was purchased from APPRYL. It was 95% isotactic and had less than 1500 ppm of additives (mainly antioxidant). The functionalized polypropylene (PP_s) was obtained from ATOCHEM and had an average of one succinic anhydride group per chain. Two molecular weights of PP_s were used: the first with M_n = 43 000 and PDI = 3.3, and the second, which was the focus of our previous study, with M_n = 22 600 and PDI = 2.7. In each case, PP_s chains were melt blended

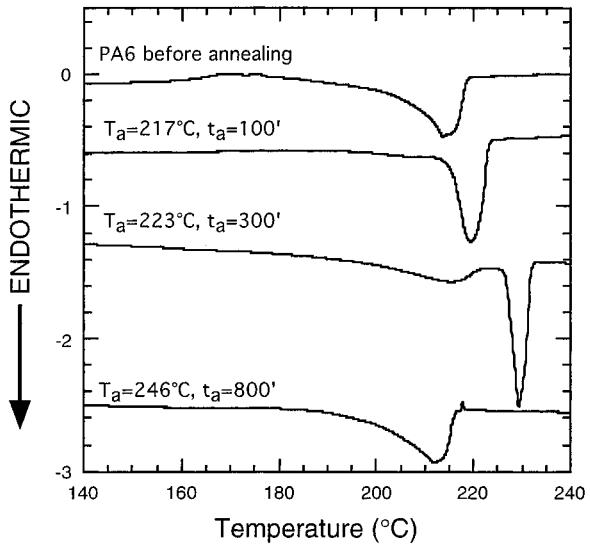

Figure 2. DSC scans of the PA6 part of joints formed under various annealing conditions (T_a is the annealing temperature and t_a the annealing time). The heating rate is 5 °C/min.

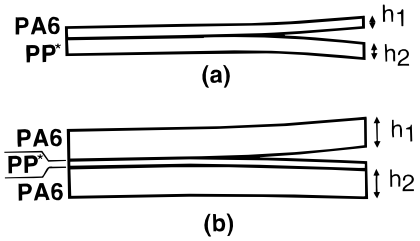

Figure 3. Schematics of the samples used for the ADCB tests: (a) simple test; (b) sandwich test.

in pure PP at a weight fraction of 5%, giving a product denoted as PP*. In the following, we will call "l-M_w PP*" and "h-M_w PP*" the PP* with respectively the lower and the higher molecular weight PP_s. All polymeric materials were available as extruded sheets of approximately 600 μm thicknesses. Formic acid (Prolabo, 98−100%), trifluoroacetic anhydride (Aldrich), and dichloromethane (Prolabo or Merck) were used as received.

Double Cantilever Beam Sample Preparation. The detailed procedure of the fabrication of the samples and of their characterization (measurement of G_c and of Σ) has been described elsewhere.[1] We just recall here what is necessary for the understanding of the present investigation. The samples were made by clamping sheets of PA6 and PP* together in an airtight, Teflon-lined mold under slight pressure, and then by heating the mold in a temperature-controlled oven at various temperatures between 185 and 223 °C, a temperature range that is above the melting temperature of PP but below that of PA6. We have checked through differential scanning calorimetric (DSC) analysis that the melting temperature of the PA6 is affected by the annealing cycle and shifted toward higher temperatures, as can be expected.[19] However, as can be seen in Figure 2, the annealing temperature remains below the melting temperature of the PA6 for all particular annealing cycles analyzed in the present paper. The thickness of each polymer side (h) was adjusted by using an appropriate number of sheets. In general, the total thicknesses for the samples ($h_{PP} + h_{PA6}$) were between 1.6 and 3.4 mm. Two geometries were used: for samples with measured fracture toughness below 140 J/m^2, we used the simple geometry shown in Figure 3a. (Samples with high energies of adhesion were thicker to increase the crack length.) Above 140 J/m^2, samples were made in the "sandwich" geometry (Figure 3b) to minimize problems due to the ductility of PP*.

The formation of copolymer occurs at the interface by reaction between the succinic acid groups on the PP_s chains

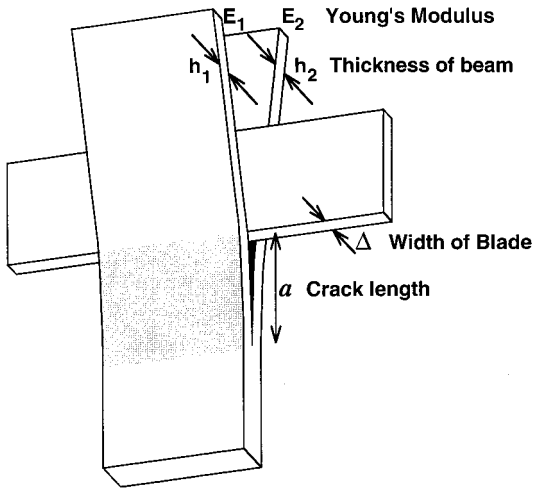

Figure 4. Schematics of the sample geometry of the ADCB test with the definition of the parameters.

and the NH_2 extremities of the PA6, which presumably results in the formation of an imide.[20] No appreciable reaction of the succinic anhydride with an amide linkage was detectable.[1] The *in situ* formation of the copolymer appears to be controlled by the diffusion of the PP_s chains to the interface,[1] and the surface density of copolymer can be adjusted by varying the annealing conditions (temperature and duration). After the prescribed annealing time, the molds were cooled to room temperature in air at a measured cooling rate of approximately 4 °C/min. All samples were stored in an atmosphere of controlled humidity for at least 24 h prior to mechanical testing, to give reproducible values for the Young's modulus of PA6.

Measurement of the Fracture Toughness. The fracture toughness (G_c) of each sample was measured using an asymmetric double cantilever beam (ADCB) test. The geometry and parameters of the ADCB test are shown in Figure 4. A blade of thickness Δ was inserted at the interface between PP* and PA6 and was pushed into the sample at a velocity of 3 μm/s. We found no dependence of the fracture toughness on the crack velocity in the range of 0.3−300 μm/s, and we therefore assumed that the measured value was equal to the critical energy release rate at zero velocity. The crack length a was measured for every millimeter that the blade advanced, by use of a video camera observing through the more transparent PP* side of the joint, or, for samples in the sandwich geometry, through the PA6. The crack length and its standard error were determined from at least 10 images. The standard deviation of the measurements was around 5%, and we estimated the accuracy of G_c to be about 10%, due to the uncertainties on the physical constants and on the thicknesses.

The ADCB test gives reliable values for G_c if two precautions are taken. First, the samples must be mechanically symmetric; that is, if the two materials have different elastic constants, the thicknesses of the two sides must be adjusted to avoid a large nonzero phase angle at the crack tip which will cause the crack to deviate into the more ductile material (PP, in our case) and result in an overestimation of the measured G_c.[21−23] We have shown[1] that, for the simple geometry, consistent values for G_c can be obtained provided the ratio of the thickness of the PP* side to the total thickness of the sample remains between 0.57 and 0.7. We checked also that the equivalent moduli used in the sandwich geometry were in agreement with the above condition: two samples made under the same experimental conditions gave the same strain energy release rate for both geometries.

Second, it is necessary to analyze correctly the data. The simple-beam equation (eq 1) often used to deduce the fracture

$$G_c = \frac{3}{8}\frac{\Delta^2}{a^4}\frac{E_1 {h_1}^3 E_2 {h_2}^3}{E_1 {h_1}^3 + E_2 {h_2}^3} \tag{1}$$

toughness from the crack length in hard materials cannot be used for ductile materials such as polymers. In eq 1, E_i and h_i are respectively the Young's modulus and the thickness of side i of the joint. (We have labeled the two sides of the joint as 1 and 2 rather than as PP* and PA6, because for the sandwich geometry, one side has both PP* and PA6.) For the simple geometry, eq 1 is not applicable when $a < 10h_{PA6}$.[1] It is only applicable for very long crack lengths relative to the thickness of a beam. On the basis of calculations by Kanninen,[24] whose central assumption was that the finite elasticity of the material ahead of the crack tip required correction factors for small crack lengths, we used the following equation:

$$G_c = \frac{3}{8}\frac{\Delta^2}{a^4}\frac{E_1 {h_1}^3 E_2 {h_2}^3}{E_1 {h_1}^3 {\alpha_2}^2 + E_2 {h_2}^3 {\alpha_1}^2} \tag{2}$$

where α_i, the correctional factor for material i, is

$$\alpha_i = \left(1 + 1.92\frac{h_i}{a} + 1.22\left(\frac{h_i}{a}\right)^2 + 0.39\left(\frac{h_i}{a}\right)^3\right)\Big/\left(1 + 0.64\frac{h_i}{a}\right) \tag{3}$$

Equation 2 gave consistent values of G_c when the ratio of the crack length to the thickness of the PA6 side was between 4 and 14.[1] All samples were made accordingly. Thicker beams are needed for samples with high fracture toughness.

Sample Preparation for the Surface Analysis. To analyze the composition of the interface between the PP* and the PA6, it was necessary to remove one of the bulk polymers from the DCB samples without disturbing the other. Since most of the energy dissipation during fracture occurs in the PP* side of the joint and we cannot readily measure the amount of PP* on a PA6 surface, it was not possible to measure the areal density of copolymers on the fracture surfaces. We needed therefore a procedure that ensured complete removal of the bulk PA6 of an unfractured surface without affecting the PP* side. The detailed procedure has been described elsewhere:[1] the majority of the bulk PA6 was dissolved in three baths of formic acid, a good solvent for PA6 that does not swell PP. A significant amount of nongrafted PA6 remained, however, at the interface after this treatment, because of hydrogen bonds between the free and copolymer chains. These hydrogen bonds were eliminated by imide formation from the amides using trifluoroacetic anhydride in the gas phase. The remaining free chains could then be easily rinsed away in dichloromethane. By soaking the sample in deionized water, the trifluoracetyl groups could be removed. This surface preparation procedure yielded a substrate of PP* with only the grafted chains of PA6 on the surface.

X-ray Photoelectron Spectroscopy (XPS). The surface density of grafted PA6 on the PP was estimated through XPS analysis. X-ray photoelectron spectra were collected on a Surfaces Science SSX-100 spectrometer using a monochromatized Al Kα_1 source ($h\nu$ = 1486.6 eV). Survey scans between 0 and 1100 eV were first taken on each sample to check for contamination of the surface. On a clean area of the sample, spectra were collected for the 1s peaks of carbon (C 1s), nitrogen (N 1s), and oxygen (O 1s) near 285, 400, and 530 eV, respectively, using a spot size of 200 × 750 μm. The pass energy on the detector was 55 eV, which gave a width of 7 eV for the detector. All spectra were collected at a takeoff angle between the sample and the detector of 35° and with an electron flood gun of 9 eV to dissipate charges in the samples. Samples were analyzed within 10 days of preparation to minimize possible oxidation of the interface. Binding energies were referenced to the hydrocarbon peak in the C 1s region at 284.8 eV. Spectra were fitted using 80% Gaussian/20% Lorentzian peak shapes and a Shirley background subtraction.[25] The reproducibility of the measurements on a single sample was approximately ±10%.

The N 1s and C 1s signals were used for determining the areal density of copolymer (Σ), assuming that the N 1s signal came exclusively from PA6 chains grafted onto the surface of the PP*, and that PA6 and PP_s chains could each only react once. Because the intensity of the C 1s signal does not vary significantly on going from pure PP to pure PA6, we normal-

ized the N 1s signals by their respective C 1s signals, to filter out fluctuations in the intensity of the X-ray source. We then assumed that the PA6 formed a homogeneous thin layer on top of the bulk PP*. The normalized nitrogen signal of a sample (N/C) is then related to the thickness of the PA6 layer (d) through eq 4, where $(N/C)_\infty$ is the normalized N 1s signal

$$\frac{(N/C)}{(N/C)_\infty} = 1 - \exp\left(-\frac{d}{\Lambda}\right) \tag{4}$$

for pure PA6; Λ accounts for the escape length of the electrons through the layer, and was estimated to be 33 Å at a binding energy of 400 eV [26] and for the takeoff angle of 35°. Using the mass density of PA6 ($\rho \approx 1$ g/cm^3), its number-average molecular weight ($M_n = 17\,000$), and Avogadro's number (N_a), we could relate the thickness d to the areal density in number of chains per unit area (Σ):

$$\Sigma = N_a \rho d / M_n \tag{5}$$

and, therefore, calculate Σ directly from the measured N 1s and C 1s signals using eq 6

$$\Sigma = -(N_a \rho / M_n)\Lambda \ln\left(1 - \frac{(N/C)}{(N/C)_\infty}\right) \tag{6}$$

Wide-Angle X-ray Scattering (WAXS). X-ray diffraction patterns were recorded using Cu Kα_1 radiation from a X-ray rotating anode generator (RU-200, Rigaku; Ltd) at 40 kV and 30 mA and equipped with a quartz curved crystal monochromator.

The geometry used is a Debye−Scherrer geometry, and patterns were recorded between 3° and 120° on a curved position detector (CPS 120, Inel). The samples were analyzed either in reflection, with an incidence angle of 1° and 3°, in order to get structural information on a depth of a few tens of microns from the surface, or in transmission to obtain a bulk structural information.

Small-Angle X-ray Scattering (SAXS). SAXS spectra were collected on a spectrometer with a rotating copper anode operating at 40 kV and 25 mA. A crystal of germanium oriented in the (111) direction was used to isolate the Cu Kα_1 line (λ = 1.5405 Å). The detector (ELPHYSE) had 512 channels and a spatial resolution of 200 μm. The distance from the sample to the detector was 80 cm. The resolution of the detector was $\Delta q = 4 \times 10^{-3}$ Å^{-1} (fwhm). The incident intensity on the sample was 6×10^6 photons/s.

From samples whose bulk PA6 had been completely rinsed away, a slice of 20 μm of PP* was removed from the side that had been in contact with the PA6. The thin slices of PP* were taken at room temperature using a SuperNova ultramicrotome (Reichert-Jung) equipped with a diamond blade of 4 mm width. The speed at which the blade went through the sample was controlled manually during the cutting. Due to limitations of the system, two slices, each with a thickness of 10 μm, had to be cut to make a 20 μm thick sample. The entire procedure was optimized to give the smallest amount of scattering at low angles in the SAXS spectra. The pieces were put in a quartz capillary for the SAXS experiments.

Differential Scanning Calorimetry (DSC). DSC was used to characterize the melting temperatures of the bulk polymers and check that the microtoming procedure did not damage or alter the crystalline structure of the samples. The DSC was a Perkin-Elmer Model DSC 7, and the samples were heated at a rate of 5 °C/min.

Results

The dependence of adhesion energy, G_c, versus the bonding time t, is reported on Figure 5, for PA6−h-M_w PP* joints prepared at four different temperatures. For all bonding temperatures, G_c increases with the bonding time and then saturates. The time at which G_c saturates depends only weakly on the bonding temperature, while the saturation value itself appears to be a very strong function of the bonding time. The most striking feature of Figure 4 is the increase in both the rate and the level of saturation of G_c at 223 °C, compared with the values at 220 °C. (These high values of G_c were measured using the sandwich geometry shown in Figure 3b.)

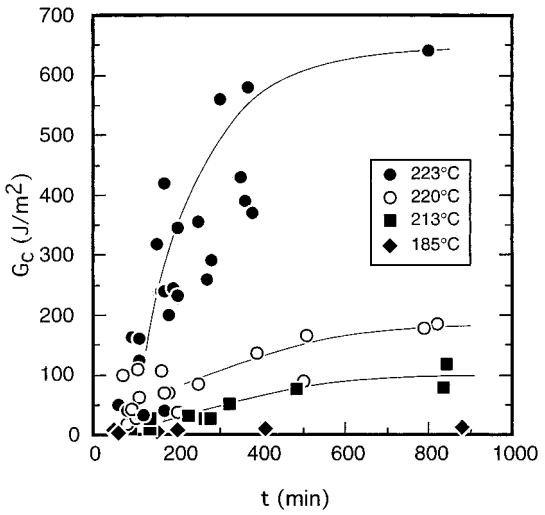

Figure 5. G_c vs annealing time t, for h-M_w PP* at four annealing temperatures.

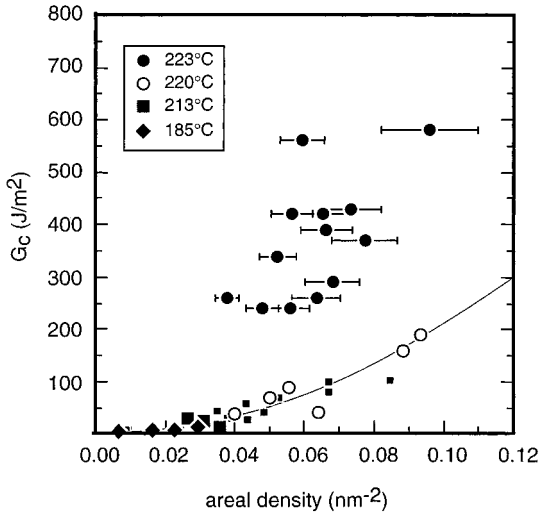

Figure 6. G_c vs areal density of connecting chains (Σ) for h-M_w PP* at four annealing temperatures. For comparison, the small filled squares are for l-M_w PP* annealed at 220 and 223 °C.

An important issue is to understand the origin of this enhanced adhesion energy. A first logical hypothesis is to think in terms of an increased areal density of copolymer chains at the interface. We measured this areal density (Σ) by XPS for each sample. The resulting dependence of G_c as a function of Σ is shown in Figure 6. Two distinct regions are clearly visible: all the data for samples made at or below 220 °C fall approximately on the same line. Data corresponding to samples made above 223 °C are well apart, with energies shifted up by a factor of approximately 4-relative to those bonded at $T \leq 220$ °C for the same Σ. Comparing Figures 5 and 6 one can conclude that if the rate and the level of saturation of G_c shown in Figure 5 increases dramatically at 223 °C, this is not because the grafting process accelerates, but because *the copolymer chains act more efficiently* at dissipating energy at the interface.

These same data are represented in a log−log plot in Figure 7. It then appears clearly that the samples made

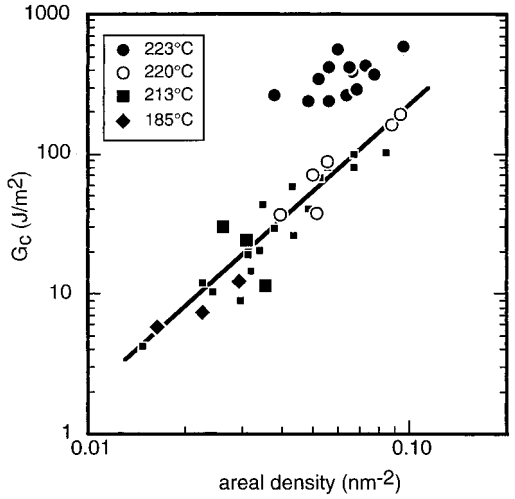

Figure 7. G_c vs Σ in a log−log plot for h-M_w PP* at four annealing temperatures. For comparison, the small filled squares are for l-M_w PP* annealed at 220 and 223 °C.

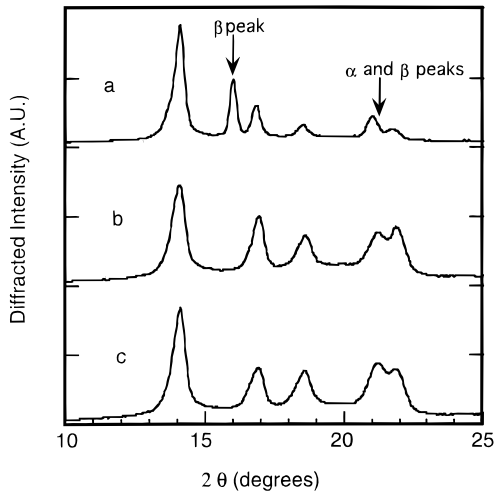

Figure 8. Off-specular WAXS spectra with a 1° incident angle for h-M_w PP* annealed at 223 °C (a), for h-M_w PP* annealed at 220 °C (b), and for for l-M_w PP* annealed at 223 °C (c).

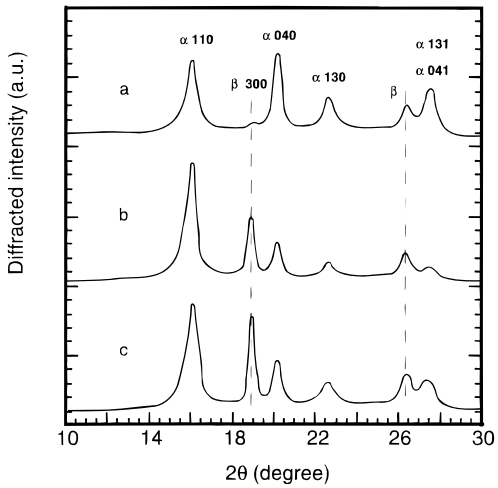

Figure 9. WAXS spectra in transmission (a) and, in off-specular reflection with a 1° incident angle (b) and with a 3° incident angle (c), for the h-M_w PP* sample annealed at 223 °C.

with h-M_w PP* at $T \leq 220$ °C have a fracture toughness proportional to Σ^2, with the same prefactor as for samples made with l-M_w PP*. However, when h-M_w PP* is bonded at $T = 223$ °C, G_c becomes much higher, implying a change in the energy dissipation mechanism associated with the fracture.

To investigate further the nature of this change in fracture mechanism when long copolymer molecules are formed at the interface, we have performed an additional analysis of the interfacial structure before and after fracture.

First, we needed to check if the plastic deformation responsible for the high G_c was indeed always occurring on the PP* side of the joint: a possible change in the crystalline structure of the PA6 close to the interface could have been produced by the annealing process occurring very close to the melting temperature, and could have led to dissipation on both the PA6 and the PP sides. Indeed, such an evolution of the crystallinity of the PA6 during annealing is certainly at the origin of the evolution of the bulk PA6 melting temperature noticed in Figure 2. The copolymer itself when present at the interface could also affect the crystallinity of the PA6[27,28] and modify the location of the fracture and the whole dissipation process. We thus analyzed by XPS the surfaces after fracture, and similarly to what had been observed for l-M_w PP*,[1] and whatever the annealing temperature including 223 °C, we found no nitrogen on the PP* side of the interface, indicating that the fracture essentially takes place inside the PP side of the joint. We can thus assume that the increase in fracture energy was therefore due to some changes in the dissipation process within the PP*.

In order to characterize further the nature of the PP* near the interface, we used wide-angle X-ray scattering (WAXS), in reflection, and small-angle X-ray scattering (SAXS) to determine the crystal structure and the macrostructure of this semicrystalline polymer close to the PP−PA6 interface.

The WAXS off-specular spectra obtained at a grazing incident angle of 1°, for different samples made with h-M_w PP*, respectively at $T = 220$ °C and $T = 223$ °C, are shown in Figure 8. The sample made at $T = 220$ °C showed exclusively the characteristic peaks of the monoclinic ($a = 6.66$ Å, $b = 10.78$ Å, $c = 6.495$ Å, and $\beta = 99.62°$) α-phase, which is the most stable crystalline phase of PP.[29] Several other samples made with h-M_w PP* below 220 °C all showed only the presence of the α-phase. When the joints were formed at 223 °C, the WAXS spectra showed, in addition to the α-phase, the presence of peaks characteristic of the β-phase of PP, best described as having a trigonal lattice ($a = b = 11.03$ Å and $c = 6.49$ Å).[30] The presence of this β-phase of PP was localized near the interface, as evidenced from the WAXS spectra as a function of the incident angle for the X-rays reported on Figure 9: as the incident angle is reduced, the peaks characteristic of the β-phase become larger relative to those of the α-phase. One can define K_x, the qualitative parameter commonly used to describe the amount of β-form in samples containing a mixture of α- and β-crystallites,[29] by

$$K_x = \frac{H_{(300)}}{H_{(300)} + (H_{(110)} + H_{(040)} + H_{(310)})} \qquad (7)$$

where $H_{(300)}$ is the height of the 300 peak for the β-form and the other $H_{(hkl)}$ are the heights of the (110), (040), and (310) peaks for the α-form in the WAXS spectra. At an angle of 1°, we estimated from our data $K_x = 26.5\%$. Values of K_x given by eq 7 have been shown to be a slight overestimation of the actual amount of β-form

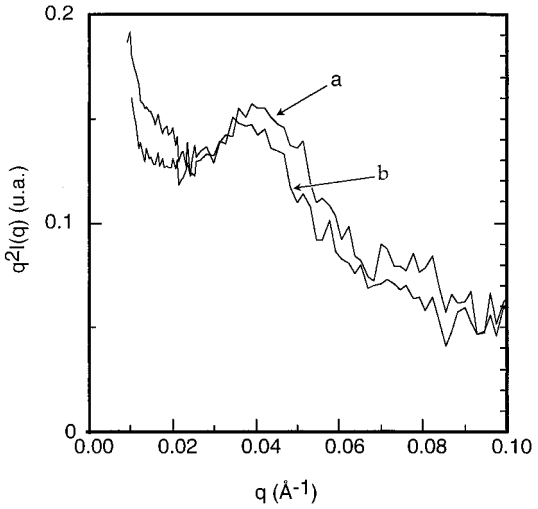

Figure 10. SAXS spectra in a $q^2I(q)$ vs q representation for h-M_w PP* annealed at 220 (a) and 223 °C (b).

by a correction factor of 0.875.[31] Using this correction factor, we found that approximately 23% of the crystalline PP was in its β-form in the region sampled by the X-ray beam.

To sum up the WAXS experiments, there is a coincidence between the regime of high fracture toughness ($\sim$200−600 J/m^2) and the presence of a polymorphic region containing both the α-phase and the β-phase of PP *at the interface* between the PP* and the PA6.

The observation of the topography of the interface using a confocal microscope (on samples that had been prepared by the rinsing procedure, rather than on samples that had been fractured) revealed another difference between a low fracture toughness sample (containing only the α-phase) and a high fracture toughness sample (with both the α- and β-phases). In a sample with only the α-phase, the roughness of the surface was measured to be $\sim$0.2 μm (rms). When both the α- and β-phases were present at the surface (for samples made with h-M_w PP* at 223 °C), the roughness of the surface increased to 0.5 μm and craterlike pits could be seen.

To measure the size of the crystallites in the various samples, we used SAXS on thin slabs of 20 μm thickness taken from the surface of the samples, using a microtome with a diamond tip. Figure 10 presents one SAXS spectra for a sample of PP* containing only the α-phase and two spectra of samples containing both phases. The three spectra show approximately the same long distance: 150 Å for the sample containing only the α-phase, and 170 and 143 Å for the two samples containing the mixture of phases. All of these results are in agreement with the value we found for the α-phase in bulk PP*.[32] These results therefore show that there is no obvious correlation between the energy of adhesion and the size of the crystallites. One should be careful, however, because the peak of the β-phase could be masked by that of the α-phase, or the procedure of microtoming could have induced a phase change in the sample. This latter hypothesis is not supported, however, by differential scanning calorimetry (DSC), which showed a small melting peak for the β-phase in samples that had been microtomed.

The DSC of the microtomed slice did reveal also the total amount of crystallinity in samples containing both forms and samples containing only the α-form were both the same at approximately 45%.

Discussion

We are now faced with two questions: First, why does the β-form of polypropylene appear only in the samples which have been heated to 223 °C , near the interface with the PA6, and only when h-M_w PP* is used? Second, could the presence of the β-form affect the copolymers at the interface in such a way that there is an increase in their efficiency to enhance adhesion by a factor of 4? Neither of these questions is answered easily. We will, however, try to propose a reasonable explanation in light of our results.

The Origin of the β-Phase. The β-form of PP is often formed in samples that either contain certain nucleating agents[15,31] or have been exposed to a thermal gradient.[30] In principle, neither of these effects was present in our system, since the PP* was free of nucleating agents and the procedure for preparing the samples did not cause a thermal gradient. Since the crystallites of the β-form of PP appeared near the interface with the PA6, an epitaxial effect is suggested. It is known that certain substrates can influence the way PP can crystallize. In particular Lotz and Wittmann have shown that PP can crystallize with a particular orientation of its lamellae when it is in contact with polyamide-11.[33] Other cases of surface-induced crystallinity have also been observed with various polyamides used as substrates.[33,34] However, to our knowledge the presence of the β-phase was never mentioned.

Clearly, the present situation is more complex, and the presence of long enough copolymer chains between PP* and PA6 appears necessary to induce the β-phase of PP. This compatibilizer can improve the continuity of the crystalline form through the surface, as has been already shown in PP−polyamide-12 alloys: the formation of copolymer chains increased the crystallization temperature of the PP phase.[35] In the same study it was also shown that the α-phase of PA6 was unfavorable for good compatibility whereas the γ-phase increased the compatibility between PA6 and PP.[35] Those results do not explain why the β-phase appears in our system, but they demonstrate the existence of some effects of molecular interactions on the crystallization process. Following this line, the formation of the PP β-phase at the interface at high annealing temperature could be due to the recrystallization of the PA6 adjacent to the interface which occurs when the temperature is increased above 220 °C. Bidaux et al. have observed in a similar system that, for temperatures lower than $\approx$225 °C, the PA6 had a 100 μm thick amorphous layer near the interphase presumably formed during the injection molding of the plate.[36] This amorphous layer recrystallized when the joining temperature increased above the melting point of PA6. In our case the PA6 side of the samples has been extruded and could presumably have an amorphous layer at the interface with PP* (although we have not been able to detect any such layer by optical microscopy on thin slabs of PA6 microtomed perpendicular to the sheets, which means that if such amorphous layer exists, it is too thin to be optically visible). Upon increasing the temperature close to the melting point of PA6, such an amorphous layer could recrystallize and upon cooling induce an epitaxial growth of the PP β- phase.

An interesting consideration is the comparison of the results obtained with the h-M_w PP* and those obtained previously on the same system with the l-M_w PP*.[1] All the samples joined at T < 220 °C give data points falling

on the same line $G_c \propto \Sigma^2$, whatever the molecular weight of the copolymer, implying that, in that temperature regime, the mechanisms of energy dissipation and failure are insensitive to the molecular weight of the connecting chains. It is however no longer the case for samples joined at $T > 220$ °C where the large reinforcement effect shown in Figures 5−7 for h-M_w PP* is not seen for l-M_w PP*.

The low temperature regime is consistent with the proposed following fracture mechanism: the dissipation occurs exclusively in the PP* side of the interface through the formation of a plastic zone, and failure occurs by chain scission of the PP part of the copolymer.[1] If the joints failed ultimately by disentanglement of the chains within the fibrils, we would have expected a dependence between the fracture toughness and the index of polymerization of the PP$_s$ (for example, $G_c \sim N^2$ as predicted by de Gennes[37]).

However, for the samples prepared above 220 °C, a higher dissipation mechanism (at a fixed Σ) is activated only when long enough copolymer chains are used. Some indications that the length of the connecting chains indeed affects significantly the crystallization process at the interface can be deduced from the WAXS analysis. For l-M_w PP*, the peaks of the β-form are quite small relative to those for the α-form, but they can still be seen by the relative increase of the peak at $2\theta = 21.1°$. However, while with h-M_w PP* the polymorphic α,β-region is present at the very surface of the sample, with l-M_w PP*, the polymorphic α,β-region is observed deeper in the bulk PP* rather than at the surface. We do not have at this stage any explanation for this fact, and additional more detailed X-ray analysis will be necessary to investigate how the long copolymer chains and the presence of PA6 close to its melting temperature can facilitate the appearance of the β-form of the PP right at the interface.

The Mechanism of Dissipation for Samples of h-M_w PP* Made at 223 °C. Although it is not entirely obvious from the data in Figure 6 that the data points are best fit by a square law, we will use Brown's model[13] as a starting point for a discussion on the dissipation mechanisms.

Using essentially several assumptions on the microstructure of the plastic zone, Brown was able to derive an equation that describes the behavior of glassy and semicrystalline polymers when the main plastic deformation mechanism ahead of the crack tip is a craze and when failure of the craze occurs by chain scission in the fibrils. His result was

$$G_c \approx \frac{\Sigma^2 f_b^{\,2} 2\pi D}{\sigma_d}\left(\frac{S_{22}}{S_{12}}\right)^{1/2}(1 - 1/\lambda) \qquad (8)$$

This is crucially dependent on the assumption that the plastic zone can be modeled as an elastic strip which can transfer stress laterally when a crack propagates through it. For glassy polymers which do deform mainly by crazing, there is a clear physical interpretation of the parameters of eq 8: f_b is the force needed to break a covalent bond, D is the craze fibril diameter, σ_d is the crazing stress, λ is the fibril extension ratio, and S_{22} and S_{12} are the tensile and shear elastic moduli of the craze, respectively. This interpretation is only possible because, for glassy polymers, the microstructure of a craze is fairly well known through various microscopy and scattering techniques.[38,39]

For semicrystalline polymers, the structure of the plastic zone in the practical range of temperatures (i.e., between T_g and T_m) is much less known, although some recent work has appeared.[18] A fibrillar structure with fairly large fibrils (tenths of microns in diameter) has been generally observed for PP[40−42] in plane strain, and it is not unreasonable to argue, as we did in ref 1, that provided the plastic zone can create a stress concentration, Brown's model can be used to interpret the evolution of the fracture toughness with the areal density of copolymer molecules formed at the interface.

The most important result reported in this paper is the large difference in the measured G_c that we found for an identical areal density of connecting chains, depending on the temperature range at which the samples are prepared. With this result in mind it is interesting to go through eq 8 and to analyze how the change of a given parameter would affect the value of G_c. Several of the parameters cannot reasonably change when the annealing temperature is changed from 220 to 223 °C: f_b, the force needed to break a bond, will remain the same since we have the same material; S_{22} and S_{12}, the shear and tensile compliances of the crazed material, respectively, should not vary much since both the α-form and the β-form become the more disordered smectic phase when the PP is highly drawn.[43,44] The three parameters that possibly could have an effect are σ_y, the yield stress of the material, D, the characteristic distance (which is no longer a distance between fibrils in the material; see ref 1), and λ, the extension ratio in the plastic zone. Although the yield stress is known to decrease somewhat on changing from the α-form to the β-form of PP, it would have to decrease to a quarter of its original value to be the only cause of the observed effect. The lower yield stress does certainly contribute to the higher fracture toughness in the samples with the β-form at the interface, but it can hardly alone explain the observed enhanced adhesion energy.

The other two parameters are harder to quantify. We previously remarked[1] that the length D estimated from the slope of G_c vs Σ^2 did not seem to correspond to the size of the fibrils. A change in the structure of the fibrillar region (or the region of plastic deformation in the PP*) might indeed have an effect on the strength.

The plastic deformation of the β-form has been investigated recently and is fairly complicated due to the several possible processes that can occur during deformation.[17,43] The crystallites can undergo two transformations:

1. The β-form can transform into the α-form. Since the α-form is more dense than the β-form, this process is often accompanied by cavitation.[17,42]

2. The β-form can also transform directly into the disordered smectic phase upon drawing.[43]

It is not clear at the moment which one of these processes would occur at the crack tip in our samples, but they could have an influence on the structure of the plastic zone and therefore influence the measured G_c. This is strongly corroborated by a recent comprehensive fracture mechanics study by Karger-Kocsis.[15] He found a work of fracture, in deeply double edge notched specimens, 4 times higher for the β-form polypropylene than for the α-form and conclusively demonstrated that this higher fracture toughness was due to the formation of a much larger plastic zone. He also showed by DSC experiments and infrared video of the plastic zone crack that the β-form PP underwent a β−α transformation which was accompanied by an increase in temperature

(of about 2 °C) and argued that the crucial factor in the improved toughness was the polymorphic transformation from a less dense to a more dense crystalline phase. We have no direct proof that such a transformation indeed takes place at the crack tip in our samples when the β-form is present at the interface, but the similarity in the observed enhanced factors of 4 in the two independent experiments is striking.

Conclusions

The results which we presented here have only begun to scratch the surface of the wide range of possible effects present in adhesion between semicrystalline polymers.

We have shown on one system, PP−PA6, that a small change in annealing temperature can induce a relatively large change in adhesion. This large change is not due to an increase in the areal density of the copolymer chains which form at the interface upon heating and act as reinforcers, but rather to a change in the efficiency of these chains at producing plastic deformation at the interface.

We found the presence of the PP β-form in all samples which were joined at a temperature above 220 °C, implying that the proximity of the melting temperature of the PA6 had an influence on the crystallization process on the PP side. However, only when high molecular weight PP chains were used as reactive connectors did the crystallites of the β-phase appear at the interface, and did their presence have a very strong reinforcing effect on the adhesion between PP* and PA6. On the basis of our knowledge of the controlling factors of the fracture toughness of an interface between polymers and of the recent results of Karger-Kocsis on the fracture mechanics of PP, it is reasonable to attribute this reinforcing effect to the presence of the β-form of PP at the interface and to the subsequent formation of a much larger plastic zone than when the α-form is present at the crack tip.

If such an effect is experimentally confirmed more conclusively, it might be an entirely novel way to think about reinforcing interfaces between semicrystalline polymers.

Acknowledgment. We are strongly indebted to ELF ATOCHEM for providing the materials used in this research and for financial support. We thank Christian Quet (Elf-Atochem Lacq) for the XPS data and Sylvie Girault (Ato Chem, Centre de Recherche, Levallois-Perret) for the X-ray analysis of the crystallinity close to the interface.

References and Notes

(1) Boucher, E.; Folkers, J. P.; Hervet, H.; Léger, L.; Creton, C. *Macromolecules* **1996**, *29*, 774−782.
(2) Fayt, R.; Jérôme, R.; Teyssié, P. *J. Polym. Sci., Part B: Polym. Phys.* **1989**, *27*, 775−793.
(3) Creton, C.; Kramer, E. J.; Hadziioannou, G. *Macromolecules* **1991**, *24*, 1846−1853.
(4) Creton, C.; Kramer, E. J.; Hui, C. Y.; Brown, H. R. *Macromolecules* **1992**, *25*, 3075−3088.
(5) Cho, K.; Brown, H. R.; Miller, D. C. *J. Polym. Sci., Part B: Polym. Phys.* **1990**, *28*, 1699−1718.
(6) Brown, H. R. *Macromolecules* **1989**, *22*, 2859−2860.
(7) Kramer, E. J.; Norton, L. J.; Dai, C. A.; Sha, Y.; Hui, C. Y. *Faraday Discuss.* **1994**, *98*, 31−46.
(8) Washiyama, J.; Creton, C.; Kramer, E. J. *Macromolecules* **1992**, *25*, 4751−4758.
(9) Char, K.; Brown, H. R.; Deline, V. R. *Macromolecules* **1993**, *26*, 4164−4171.
(10) Brown, H. R.; Char, K.; Deline, V. R.; Green, P. F. *Macromolecules* **1993**, *26*, 4155−4163.
(11) Dai, C.-A.; Dair, B. J.; Dai, K. H.; Ober, C. K.; Kramer, E. J.; Hui, C. Y.; Jelinski, L. W. *Phys. Rev. Lett.* **1994**, *73*, 2472−2475.
(12) Creton, C.; Brown, H. R.; Deline, V. R. *Macromolecules* **1994**, *27*, 1774−1780.
(13) Brown, H. R. *Macromolecules* **1991**, *24*, 2752−2756.
(14) Washiyama, J.; Kramer, E. J.; Creton, C.; Hui, C. Y. *Macromolecules* **1994**, *27*, 2019−2024.
(15) Karger-Kocsis, J. *Polym. Eng. Sci.* **1996**, *36*, 203−210.
(16) Plummer, C. J. G.; Menu, P.; Cudré-Mauroux, N.; Kausch, H. H. *J. Appl. Polym. Sci.* **1995**, *55*, 489−500.
(17) Zhang, X.; Shi, G. *Polymer* **1994**, *35*, 5067−5072.
(18) Plummer, C. J. G.; Kausch, H. H. *Macromol. Chem. Phys.* **1996**, *197*, 2047−2063.
(19) Ellis, T., *Polymer* **1988**, 29, 2015.
(20) Maréchal, P.; Coppens, G.; Legras, R.; Dekoninck, J. *J. Polym. Sci., Part A: Polym. Chem.* **1995**, *33*, 757−766.
(21) Brown, H. R. *J. Mater. Sci.* **1990**, *25*, 2791−2794.
(22) Xiao, F.; Hui, C. Y.; Kramer, E. J. *J. Mater. Sci.* **1993**, *28*, 5620−5629.
(23) Xiao, F., Hui, C. Y.; Washiyama, J.; Kramer, E. J. *Macromolecules* **1994**, 27, 4382
(24) Kanninen, M. F. *Int. J. Fract.* **1973**, *9*, 83−92.
(25) Shirley, D. A. *Phys. Rev. B* **1972**, *5*, 4709.
(26) Laibnis, P. E.; Bain, C. D.; Whitesides, G. M. *J. Phys. Chem.* **1991**, *95*, 7017−7021.
(27) Moon, H. S.; Ryoo, B.-K.; Park, J.-K., *J. Polym. Sci., Polym. Phys. Ed.* **1994**, *32*, 1432.
(28) Tang, T.; Huang, B. *J. Appl. Polym. Sci.* **1994**, 53, 355.
(29) Turner-Jones, A.; Aizlewood, J. M.; Beckett, D. R. *Makromol. Chem.* **1964**, *75*, 134−159.
(30) Meille, S. V.; Ferro, D. R.; Brückner, S.; Lovinger, A. J.; Padden, F. J. *Macromolecules* **1994**, *27*, 2615−2622.
(31) Jacoby, P.; Bersted, B. H.; Kissel, W. J.; Smith, C. E. *J. Polym. Sci., Part B: Polym. Phys.* **1986**, *24*, 461−491.
(32) Boucher, E. Sciences Physiques Thesis, Université Paris VI, 1995.
(33) Lotz, B.; Wittmann, J. C. *J. Polym. Sci. B Polym. Phys.* **1986**, *24*, 1559−1575.
(34) Chatterjee, A. M.; Price, F. P. *J. Polym. Sci., Polym. Phys. Ed.* **1975**, *13*, 2369−2383.
(35) Tang, T.; Li, H.; Huang, B. *Macromol. Chem. Phys.* **1994**, *195*, 2931−2945.
(36) Bidaux, J. E.; Smith, G. D.; Bernet, N.; Manson, J. A.; Hilborn, J. *Polymer* **1996**, *37*, 1129−1136.
(37) de Gennes, P. G. *Europhys. Lett.* **1991**, *15*, 191−196.
(38) Kramer, E. J. *Adv. Polym. Sci.* **1983**, *52/53*, 1−56.
(39) Kramer, E. J.; Berger, L. L. *Adv. Polym. Sci.* **1990**, *91/92*, 1−68.
(40) Jang, B. Z.; Uhlmann, D. R.; Vander Sande, J. B. *Polym. Eng. Sci.* **1985**, *25*, 98−104.
(41) Olf, H. G.; Peterlin, A. *J. Polym. Sci., Polym. Phys. Ed.* **1974**, *12*, 2209−2251.
(42) Olf, H. G.; Peterlin, A. *Macromolecules* **1973**, *6*, 470−472.
(43) Chu, F.; Yamaoka, T.; Ide, H.; Kimura, Y. *Polymer* **1994**, *35*, 3442−3448.
(44) Kammer, H. W.; Kummerloewe, C.; Greco, R.; Mancarella, C.; Martuscelli, E. *Polymer* **1988**, *29*, 963−969.

MA961105I